Vol 17 No 1, January 2008
1674-1056/2008/17(01)/0328-07

Chinese Physics B

© 2008 Chin. Phys. Soc.
and IOP Publishing Ltd

Phase-sensitive fat suppression steady-state free procession sequence with phase correction*

Zu Zhong-Liang(俎中良)[a], Zhou Kun(周 堃)[a], Zhang Shi-Gang(张仕刚)[b], Gao Song(高 嵩)[a)c)], and Bao Shang-Lian(包尚联)[a)†]

[a)] *Beijing City Key Laboratory of Medical Physics and Engineering, Peking University, Beijing* 100871, *China*
[b)] *Siemens Mindit MRI Center, Shenzhen* 518112, *China*
[c)] *Medical Physics Department, Health Science Center of Peking University, Beijing* 100083, *China*

(Received 6 February 2007; revised manuscript received 29 April 2007)

Robust and fast fat suppression is a challenge in balanced steady-state free precession (SSFP) magnetic resonance imaging. Although single-acquisition phase-sensitive SSFP can provide fat-suppressed images in short scan time, phase errors, especially spatially-dependent phase shift, caused by a variety of factors may result in misplacement of fat and water voxels. In this paper, a novel phase correction algorithm was used to calibrate those phase errors during image reconstruction. This algorithm corrects phase by region growing, employing both the magnitude and the phase information of image pixels. Phantom and *in vivo* imagings were performed to validate the technique. As a result, excellent fat-suppressed images were acquired by using single-acquisition phase-sensitive SSFP with phase correction.

Keywords: steady-state free precession, fat suppression, phase-sensitive, phase correction
PACC: 8760I, 3325D

1. Introduction

Balanced steady-state free precession (SSFP) sequences (i.e., TrueFISP, FIESTA, balanced-FFE) provide a relatively high signal and high contrast magnetic resonance (MR) imaging in short scan times.[1,2] Such sequences were widely used in recent years. Examples of such applications include cardiac imaging,[3,4] angiography,[5,6] and abdominal imaging.[7] However, lipid protons, which exhibit an intense signal, obscure visualization of other structures.[8] Therefore, a separation or suppression of fat signals is essential.

Recently, several fat-suppressing techniques for SSFP sequences have been presented. Linear-combination SSFP[9] and multipoint Dixon techniques combined with SSFP[10,11] separate fat and water in post-processing procedure, but they double the acquisition time, and thus result in a sacrifice of imaging efficiency. Fluctuating-equilibrium MR,[12] alternating time of repetition (TR) balanced SSFP,[13] oscillating SSFP,[14] and SLIMFEST[15] produce low fat signal. The drawbacks of those techniques are that very short TR and increased total acquisition time are required to achieve the desired profile. Spectral or fat saturated SSFP[16] offers fat-suppressed images with the insertion of a spectral selective saturation pulse. Although the total imaging time is not increased so much, the technique suffers from transient artifacts and less reliable fat suppression.[17]

Single-acquisition phase-sensitive SSFP separates fat and water without additional scan time.[18] The formation of the echo is to occur concurrently for both water and fat exactly halfway between radiofrequency (RF) pulses, and the refocused magnetization vectors of fat and water have a 180° phase difference depending on appropriate selection of the repetition time and the centre frequency. Therefore, the image pixels can be separated into water and fat images based on the sign of the signal. However, misplacement of fat and water voxels may occur which results from a variety of phase errors caused by RF receiver coil, complex RF receiver filters, timing mismatches between gradients and acquisition, inadequate gradient compensation or RF penetration.[19] So the separation of the intrinsic signal phase from these phase errors is a challenge in phase-sensitive SSFP image reconstruction. In this

*Project partially supported by the National Natural Science Foundation of China (Grant Nos 10527003 and 60672104), the State Key Development Program for Basic Research of China (Grant No 2006CB705700-05), Joint Research Foundation of Beijing Education Committee (Grant No SYS100010401) and Beijing Natural Science Foundation (Grant No 3073019).
†E-mail: bao@pku.edu.cn

paper, we propose the use of a novel post-processing phase-correction algorithm for phase errors removal in phase-sensitive SSFP. The phase-correction method corrects phase errors by region-growing, which employs both the magnitude and the phase information of image pixels.[20] We demonstrate the feasibility of separating fat and water signals with phase-sensitive SSFP under the effect of phase errors by using the post-processing phase correction method.

2. Theory

2.1. Phase-sensitive SSFP

The conventional balanced SSFP[1,2] sequence consists of a train of RF pulses with flip angle α equidistantly spaced by TR and alternating in sign, as shown in Fig.1.

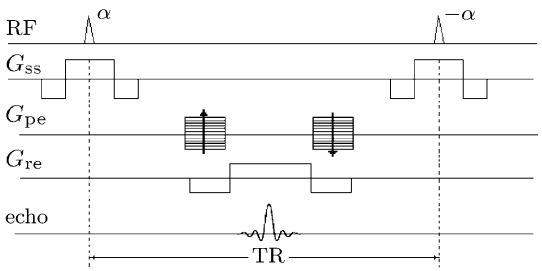


Fig.1. A standard SSFP pulse sequence consists of excitation pulses spaced TR apart, which alternate in sign. All imaging gradients are rewound over a repetition.

Imaging gradients are applied on three axes with vanishing zeroth moment in one repetition period. The SSFP signal with constant flip angle at an echo time (TE) for a species with an off-resonance frequency f can be written as:[21]

$$M(\mathrm{TE},\beta)=\frac{a\mathrm{e}^{-\mathrm{i}\beta}+b}{c\cos\beta+d}\mathrm{e}^{\mathrm{i}2\pi f\mathrm{TE}}. \tag{1}$$

Where $\beta(=2\pi f\mathrm{TR})$ is the precession phase of a species relative to RF pulses with a off-resonance frequency of f over a repetition and

$$\begin{aligned}
a&=E_2(E_1-1)\sin a,\\
b&=(1-E_1)\sin a,\\
c&=E_2(E_1-1)(1+\cos\beta),\\
d&=1-E_1\cos a-(E_1-\cos\beta)E_2^2,\\
E_1&=\exp(-\mathrm{TR}/T_1),\\
E_2&=\exp(-\mathrm{TR}/T_2).
\end{aligned}$$

Where T_1 is the spin–lattice relaxation time, and T_2 is the spin–lattice relaxation time. For SSFP signal with alternating flip angle, the above equation should be modified. As the phase of RF pulses increases π over a repetition, β should be $2\pi f\mathrm{TR}-\pi$. Usually $\mathrm{TR}<<T_1$, T_2, and thus $E_1\approx 1-\mathrm{TR}/T_1$, $E_2\approx 1-\mathrm{TR}/T_2$ and $a\approx -\mathrm{TR}/T_1(1-\mathrm{TR}/T_2)\sin a$, $b\approx \mathrm{TR}/T_1\sin a$. The phase of the signal can then be approximated by:

$$\arg(M(\mathrm{TE},\beta))=\arg((1-\mathrm{e}^{-\mathrm{i}\beta})\mathrm{e}^{\mathrm{i}2\pi f\mathrm{TE}}). \tag{2}$$

Where $\arg(\ldots)$ represents argument operation. Let $\tau=\mathrm{TE}-\mathrm{TR}/2$ (therefore $-\mathrm{TR}/2<\tau<\mathrm{TR}/2$), and by some simple manipulations we can write the phase as

$$\begin{aligned}
\arg(M(\mathrm{TE},\beta))&=\arg((1-\mathrm{e}^{-\mathrm{i}\beta})\mathrm{e}^{\mathrm{i}2\pi f(\mathrm{TR}/2+\tau)})\\
&=\arg((1-\mathrm{e}^{-\mathrm{i}\beta})\mathrm{e}^{\mathrm{i}2\pi f(\mathrm{TR}-\pi)/2}\mathrm{e}^{i(2\pi f\tau+\pi/2)})\\
&=\arg(2\mathrm{i}\sin(\beta/2))+2\pi f\tau+\pi/2\\
&=\begin{cases}2\pi f\tau & -n/(2\mathrm{TR})<f<n/(2\mathrm{TR}),\\ \pi+2\pi f\tau & -(2n+1)/(2\mathrm{TR})<f<-n/(2\mathrm{TR}),\end{cases}\quad (n=\cdots,-1,0,1,\cdots).
\end{aligned} \tag{3}$$

Therefore, when $\mathrm{TE}=\mathrm{TR}/2$, the spin isochromats at similar resonant frequencies show spin-echo-like phase coherence at eight 0 or π relative to RF pulses within different off-resonance frequency ranges, under the assumption of $\mathrm{TR}<<T_1$, T_2. The simulated SSFP signal amplitude and phase profile at $\mathrm{TE}=\mathrm{TR}/2$ is shown in Fig.2. Since water and fat have different resonant frequencies, appropriate choice of TR and centre frequency results in water and fat having opposite signs. Therefore, water or fat images can be generated

by simply choosing the positive or negative signal.[18] Phase-sensitive SSFP is a method which separates fat and water based on the sign of the signal.

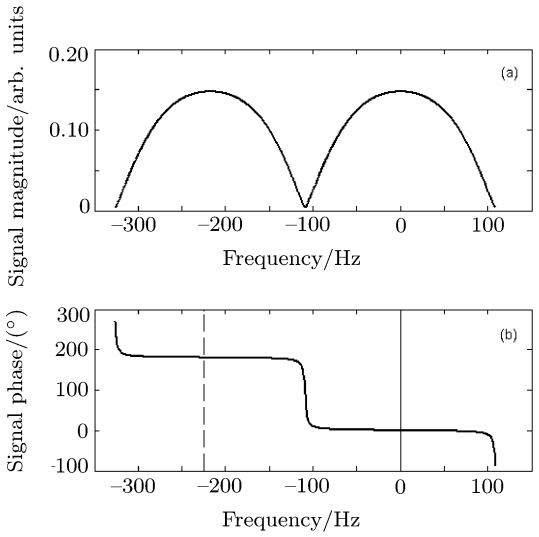


Fig.2. (a): SSFP signal magnitude for TE = TR/2 = 4.6ms and a 60° flip angle for T_1/T_2 = 900/100ms. (b): The signal phase is flat and relatively independent of off-resonance frequency. Solid line and dashed line show that water and lipid peaks are centred in adjacent signal bands.

2.2. Spatially-dependent phase errors

Since SSFP signal exhibits spin-echo-like behaviour, phase dispersion caused by the field inhomogeneity or susceptibility variations can be refocused at time TR/2.[22] However, there are still some other factors which contribute to phase errors.[19] RF receiver coil, especially surface or surface-phased-array coils, can introduce a spatial dependence into the phase of the signal received. RF receiver filters, which are used to eliminate high frequency noise, can add a frequency-dependent phase shift to the signal due to the complex nature of the transfer function of the filter. The frequency-dependent phase shift will appear to be spatially dependent in the image space. Inadequate gradient compensation and timing mismatches between gradients and acquisition always causes linear phase shift in k-space, which is also a kind of spatially-dependent phase shift in the image space. In high field imaging, RF penetration effect is unavoidable, which is another source that cause spatially-dependent phase shift.

2.3. Phase correction algorithm

Hargreaves *et al*[18] applied a simple phase correction method in their work, in which a best fit line was first found on a scatter plot, and then was rotated to remove the best-fit phase. However, only system phase can be removed through the best-fit method. When surface or surface-phased-array coil is used or RF penetration effect is significant, spatially-dependent phase errors occur which results in misplacement of fat and water voxels. The Fourier transform of the time-domain acquired in a SSFP sequence can be expressed in general as:

$$S(m,n) = I(m,n)\mathrm{e}^{\mathrm{i}\varphi(m,n)}, \tag{4}$$

$$\varphi(m,n) = \phi_0(m,n) + \phi(m,n) + \theta(m,n). \tag{5}$$

Where the signal magnitude of a given pixel is represented by $I(m,n)$; m and n are the spatial indices of the pixel; $\varphi(m,n)$ is the total phase shift. $\phi_0(m,n)$, which can only take a value of either 0 or π, is the intrinsic signal phase depending on whether water or fat is dominant in the pixel. $\phi(m,n)$ denotes the spatially-dependent phase errors resulting from a variety of factors; and $\theta(m,n)$ is the system phase, which is typically assumed to be space independent.

To eliminate the spatially-dependent phase errors, as well as the system phase, a novel phase correction algorithm[20] was used, which calibrated phase errors by region-growing, employing both the magnitude and phase information of image pixels. Specifically, spatial gradients of the signal phase along the x- and y-axes, respectively, are first calculated as follows:

$$G_x(m,n) = \left|\arg(S(m,n)\cdot S^*(m+1,n))\right|, \tag{6}$$

$$G_y(m,n) = \left|\arg(S(m,n)\cdot S^*(m+1,n))\right|, \tag{7}$$

in which $||$, and * represent the magnitude, and complex conjugate operations, respectively. $S(m,n)$ represents the phase vector of a pixel. All pixels with a value of more than $\pi/2$ in G_x and G_y are replaced with $\pi - G_x$ and $\pi - G_y$, respectively, in order to eliminate possible abrupt changes due to the intrinsic phase factor $\mathrm{e}^{\mathrm{i}\phi_0(m,n)}$. However, instead of sharp phase change (approximately π), smoother phase variation always occurs at the boundary between fat and water dominant regions in practice.[23] Therefore, to remove the assumption of the sharp phase change, a low-pass filter was applied to the phase gradient map before region growing.

For the actual region-growing process, first, a series of numbered pixel stacks are created and initialized to zero. The initial seed is selected randomly from the image and placed on any pixel stack. Second, each of the four nearest neighbour pixels of the seed is visited, except those visited before, and placed onto one of the stacks in an order depending on the value of G_x or G_y. Third, during the region growing, a boxcar average of phase is calculated by using both the phase and amplitude of the signals from the previously determined pixels over a region defined by the boxcar centred at the seed pixel and used as the reference to guide the selection of the signal direction for the seed. The reference is weighted more heavily with pixels of higher amplitude, because the signal phase of these pixels is usually more reliable than the signal phase of the pixels of lower amplitude. If the angular difference between the reference and the seed pixel is less than $\pi/2$ $\varphi(m,n)$ takes the value of 0, otherwise, $\varphi(m,n)$ takes the value of π. The above region-growing process is repeated, with a new seed pixel in the pixel stacks selected each time, until all the pixel stacks are visited. By using the above phase correction algorithm, slowly varying phase errors caused by a variety of factors can be removed while phase shift between fat and water is preserved.

3. Materials and methods

Water and lipid (soybean oil) phantoms were used to verify fat/water separation. Experiments were conducted with a Siemens Symphony 1.5T MR scanner (Siemens, Erlangen, Germany) by using a TrueFISP pulse sequence and a six-channel phased-array coil. The imaging parameters were a 60° flip angle, TR/TE = 4.6/2.3ms, 256 × 256 matrix, 30 cm ×30 cm field of view and 5mm slice thickness. To ascertain *in vivo* applicability of the technique, fat-suppressed abdominal imaging was performed on a healthy volunteer with a two-channel phased-array coil. The imaging parameters were similar to that used in phantom experiment.

Raw data were first collected from the scanner, and then image reconstruction with phase correction was performed offline on an IBM-compatible PC with an AMD processor (Athlon 3500+) operating on the Microsoft Windows XP platform. The algorithm was implemented in Matlab 6.5 (The Math Works, Natick, MA). The width of the boxcar was selected as 7 × 7, which compromised the limitation of fast local magnetic field changes and the immunity to local phase fluctuation. A total of nine pixel stacks were used, each of which covered an angular range of 10°. All the processing took approximately 5s for a 256 × 256 image with data from one channel. By removing these phase errors an image with positive and negative pixels can be achieved. The image pixels were then separated into water and fat images based on the sign of the signal.

4. Results

4.1. Phantom study

Data of a phantom of water and fat were acquired. The complex image data from one channel are scatter-plotted in Fig.3. The phase of the image data deviates greatly in Fig.3(a), while the points are well distributed along the real axis in Fig.3(b). All images in Fig.4 show the phantom images reconstructed from data acquired with 6 channels except Figs.4(d) and 4(h) which use data only from one channel. Failed separation of fat and water can be seen from Figs.4(b) and (4f), while fat signal in Fig.4(g) is separated from water in Fig.4(c) successfully. By removing the system phase and spatially-dependent phase errors, phase-sensitive SSFP provides excellent fat-suppressed image. After phase correction, the real part of the complex data can be used to reconstruct an image with enhanced contrast between fat and water in Figs.4(e). Figures 4(d) and 4(h) show the phase map before and after phase correction, respectively. Serious phase shift can be seen in Fig.4(d), while homogeneous phase was achieved in either fat phantom or water phantom in Fig.4(h). The white points in the water phantom are a typical consequence of the wrapping effect. Approximate 180° phase difference can be found between fat and water after phase correction.

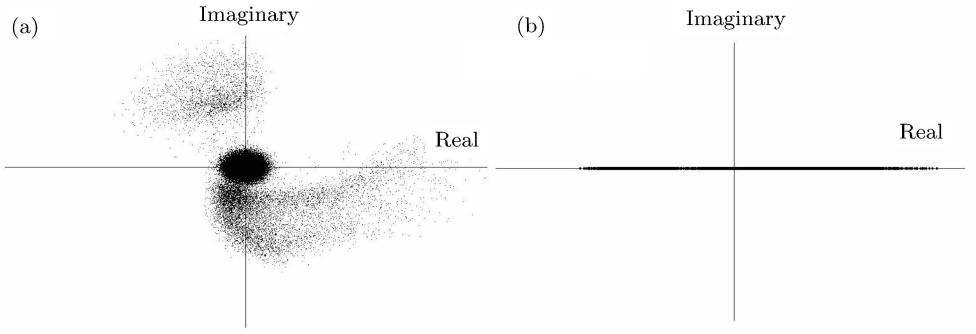


Fig.3. Scatter plot of complex image pixels. (a) before phase correction; (b) after phase correction.

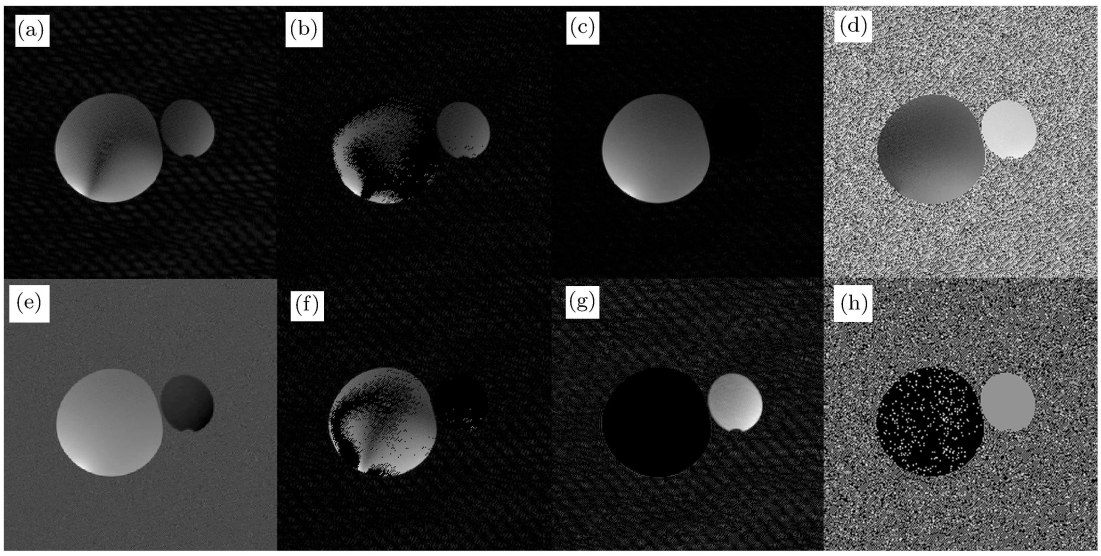


Fig.4. Phantom images: (a) combined image before correction; (b) water image before correction; (c) water image after correction; (d) phase map before correction; (e) combined image after correction; (f) fat image before correction; (g) fat image after correction; (h) phase map after correction.

4.2. *In vivo* study

Figures 5 (a–f) show the abdominal images from one male subject (27 years old). The lipid signal is well attenuated in the single-acquisition phase-sensitive SSFP with phase correction. In particular, lipids that are present around the organs and below the skin are nearly totally suppressed. This artifact free water image is achieved in a reduced total scan time, which indicates that this fat suppression technique is particularly valuable for applications that are sensitive to scan time, such as abdominal imaging, cardiac CINE imaging and pediatric imaging, where increased scan time always leads to motion artifact.

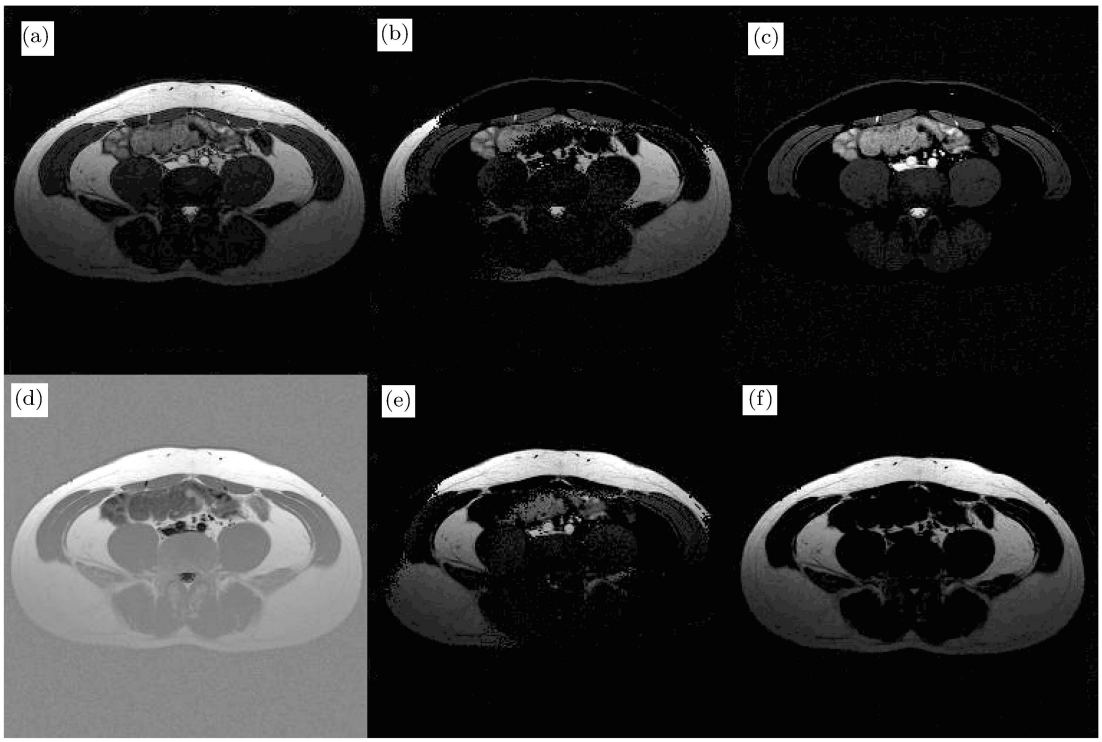


Fig.5. Abdominal images: (a) combined image before correction; (b) water image before correction; (c) water image after correction; (d) combined image after correction; (e) fat image before correction; (f) fat image after correction.

5. Discussion

Phantom and *in vivo* studies show that the separation of fat and water fails in single-acquisition phase-sensitive SSFP without phase errors correction. To solve this problem, Hargreaves *et al* [18] used a GE linear extremity transmit-receive coil (GE Medical Systems, Waukesha, WI), which introduced little phase shift. In addition, the images must be reconstructed by first using a standard Fourier reconstruction to ensure that there was no linear phase shift, and a best-fit method was also used to remove system phase. In this work, a novel phase correction algorithm was applied to eliminate all the phase errors in one step during image reconstruction. Therefore, not only the phase correction procedure is simplified, but also any coil can be used in single-acquisition phase-sensitive SSFP. The method is also useful for application at high field strength, where the RF penetration is significant.

Some previously proposed phase correction methods[24−27] use only the phase information of a neighbouring pixel or are not based on region-growing scheme, and therefore are subjected to substantial uncertainty for pixels with artifacts or low SNR, while the phase correction algorithm used here is a robust and efficient technique compared with those methods. An advantage of using the region-growing scheme is that an optimal growth path, which follows a minimum angular difference between neighbouring pixels, is chosen to avoid local phase fluctuations However, although the novel algorithm is not sensitive to local phase fluctuations, all the post-processing phase-correction methods are based on a hypothesis that the actual spatial variation of phase errors in SSFP image is generally slow.

In this study, a boxcar kernel size of 7×7 pixels was chosen to mitigate the phase fluctuation caused by pixels with low signals or artifacts. However, larger size of the boxcar is limited by fast local magnetic field changes. As the number of the pixel stacks is unimportant in practice, and an angular range of 15° for each stack is enough to provide consistent results,[20] nine pixel stacks with an angular range of 10° for each stack were created. As a result, an optimal growth path, which followed a minimum angular difference between neighbouring pixels, was sorted out.

As a rapid and efficient fat suppression MR imaging method, single-acquisition phase-sensitive SSFP,

however, has its limitation compared with other fat suppression SSFP imaging methods.[9−16] First, the SNR of the water image is not as good as that in other fat suppression SSFP imagings, which possibly results from the dynamic range of the receiver or some signal cancellation if both fat and water are in a voxel.[18] However, with the development of improved receiver systems, the dynamic range performance will be improved. Second, when fat and water occupy a single voxel, partial-volume effect occurs. Therefore, the method is appropriate for high-spatial-resolution imaging and particular imaging applications, such as angiography, in which fat and water do not always occupy the same voxels. Recently, several works are attempting to solve the problem of partial-volume effect[28−30] in single acquisition fat suppression SSFP, and the results are encouraging.

6. Conclusions

In this paper, we have shown the feasibility of applying a novel phase correction algorithm in single-acquisition phase-sensitive SSFP for phase errors calibration during image reconstruction. Excellent fat and water separation was acquired without using any specific coil or any care taken to ensure the absence of linear phase shift. Applications of the technique under great field inhomogeneity are currently under way, which include not only clinical usages, but also petroleum well detection.[31]

Acknowledgments

The authors are grateful to Professor Ma Jingfei (M. D. Anderson Cancer Center, University of Texas) and Professor Hargreaves Brian (Lucas MRS center, Stanford University) for valuable discussion.

References

[1] Carr H Y 1985 *Phys. Rev.* **112** 1693
[2] Oppelt A, Graumann R, Barfuss H, Fischer H, Hartl W and Shajor W 1986 *Electromedica* **54** 15
[3] Lee V S, Resnick D, Bundy J M, Simonetti O P, Lee P and Weinreb J C 2002 *Radiol.* **222** 835
[4] Jung B A, Hennig J and Scheffler K 2002 *Magn. Reson. Med.* **48** 921
[5] Carr J C, Simonetti O, Bundy J Li D B, Pereles S and Finn J P 2001 *Radiol.* **219** 828
[6] Pereles F S, McCarthy R M, Baskaran V, Carr J C, Kapoor V, Krupinski E A and Finn J P 2002 *Radiol.* **223** 270
[7] Borthne A S, Dormagen J B, Gjesdal K I, Storaas T, Lygren I and Geitung J T 2003 *Eur. Radiol.* **13** 100
[8] Haacke E M, Wielopolski P A, Tkach J A and Modic M T 1990 *Radiol.* **175** 545
[9] Vasanawala S S, Pauly J M and Nishimura D G 2000 *Magn. Reson. Med.* **43** 82
[10] Reeder S B, Alley M T, Pelc N J and Gold G E 2003 *Am. J. Roentgenol.* **180** 357
[11] Huang T Y, Chung H W, Wang F N, Ko C W and Chen C Y 2004 *Magn. Reson. Med.* **51** 243
[12] Vasanawala S S, Pauly J M and Nishimura D G 1999 *Magn. Reson. Med.* **42** 876
[13] Leupold J, Hennig J and Scheffler K 2006 *Magn. Reson. Med.* **55** 557
[14] Overall W R, Nishimura D G and Hu B S 2003 *Magn. Reson. Med.* **50** 550
[15] Hardy C J and Dixon W T 2002 *Proc. ISMRM* USA p473
[16] Scheffler K, Heid O and Hennig J 2001 *Magn. Reson. Med.* **45** 1075
[17] Hargreaves B A, Vasanawala S S, Pauly J M and Nishimura D G 2001 *Magn. Reson. Med.* **4**6 149
[18] Hargreaves B A, Vasanawala S S, Nayak K S, Hu B S and Nishimura D G 2003 *Magn. Reson. Med.* **50** 210
[19] McVeigh E R, Bronskill M J and Henkelman R M 1986 *Med. Phys.* **13** 806
[20] Ma J 2005 *Magn. Reson. Med.* **53** 904
[21] Sekihara K 1978 *IEEE Trans. Med. Imaging* **MI6** 157
[22] Scheffler K and Hennig J 2003 *Magn. Reson. Med.* **49** 395
[23] Schmidt M A and Fraser K M 2006 *Proc. ISMRM* USA p2401
[24] Borrello J A, Chenevert T L and Aisen A M 1990 *Magn. Reson. Med.* **14** 56
[25] Xiang Q S 1996 *J. Magn. Reson. Imaging* **6** 775
[26] Ma J 1999 *Proc. ISMRM* USA p1652
[27] Ji J, Ying L, Ma J, Munson D C and Liang Z P 2003 *Proc. ISMRM* Canada p1069
[28] Lu A, Brodsky E, Grist T M and Block W F 2005 *Magn. Reson. Med.* **53** 692
[29] Yu H, Reeder S B, Markl M and Pelc N J 2004 *Proc. ISMRM Japan* p263
[30] Gurney P, Hargreaves B and Nishimura D 2004 *Proc. ISMRM Japan* p2133
[31] Zhang B D, Wang W D, Song X Y, Zu D L, Lu H Y and Bao S L 2003 *Acta Phys. Sin.* **52** 1143 (in Chinese)